TECHNICAL PAPER

Plane wave propagation in a piezo-thermoelastic rotating medium within the dual-phase-lag model

Ethar A. A. Ahmed[1] · M. S. Abou-Dina[1] · A. F. Ghaleb[1]

Abstract

We investigate the effect of rotation on plane wave propagation in a half-space of a piezo-thermoelastic material within the frame of dual-phase-lag model. Normal mode technique is used to obtain analytic expressions for the displacement components, temperature and stress components. Numerical results for the quantities of practical interest are given in the physical domain and illustrated graphically. Comparison is carried out between the results predicted by the dual-phase-lag model and Lord–Shulman theory, in the presence or absence of rotation. It is believed that the present results may be useful in the design and construction of different pyro/piezoelectric devices, such as gyroscopes and sensors.

List of symbols

u_i	The mechanical displacement
T	Absolute temperature
σ_{ij}	Stress tensor
E_i	Electric field
C_{ijkl}	Elastic stiffness tensor
$\in_{ij}$	The dielectric moduli
τ_θ	Phase lag of temperature gradient
K_{ij}	Heat conduction tensor
C_T	Specific heat at constant strain
α_1, α_3	Coefficients of linear thermal expansion
$v_p = \sqrt{\frac{1}{\rho} C_{11}},$	Longitudinal wave velocity
φ	Electric potential
ε_{ij}	Strain tensor
β_{ij}	Thermoelastic tensor
D_i	Electric displacement
e_{ijk}	Piezoelectric tensor
p_i	Pyroelectric moduli
τ_q	Phase lag of the heat flux
T_0	Reference temperature
ρ	Mass density

✉ Ethar A. A. Ahmed
  ethar_ahmed54@yahoo.com

1   Department of Mathematics, Faculty of Science, Cairo
    University, Giza 12613, Egypt

1 Introduction

The design and construction of piezoelectric gyroscopes and other rotating sensors have important applications in technology. The study of the effects of rotation on the propagation of waves in piezo-thermoelastic media has been extensively studied in the past two decades.

The theory of thermo-piezo-electricity was first proposed by Mindlin (1974). Ahmed et al. (2019) applied dual-phase-lag model to study the effect of gravity on piezo-thermoelastic half-space medium by using normal mode analysis method. Othman and Ahmed (2015) investigated the effect of rotation of a piezo-thermoelastic medium based on three theories (CT, L–S, G–L). Othman and Ahmed (2016) used normal mode analysis method to investigate the influence of the gravitational field on a piezo-thermoelastic rotating medium with G–L Theory. Schoenberg and Censor (1973) investigated an elastic waves in rotating media. Alshaikh (2012) presented the mathematical modelling for studying the influence of the initial stresses and relaxation times on reflection and refraction waves in piezothermoelastic half-space. The effects of piezoelectricity and piezomagnetism on the surface wave velocity of magneto-electroelastic solids has been investigated by Li and Wei (2014). Othman (2004) studied the effect of rotation on plane waves in generalized thermoelasticity with two relaxation times. Othman et al. (2013) studied the influence of gravity field and rotation on a generalized thermoelastic medium using dual-phase-lag model. Kumar et al. (2018) discussed the reflection of plane waves at a free surface of orthotropic micropolar

piezothermoelastic medium. Sharma and Kumar (2000) studied the plane harmonic waves in piezo-thermoelastic materials. Abbas and Zenkour (2014) used a finite element method to study dual-phase-lag model on thermoelastic interactions in a semi-infinite medium subjected to a ramp-type heating. Abou-Dina et al. (2017) studied the model of nonlinear thermo-electroelasticity in extended thermo-electroelasticity in extended thermoelasticity. Mahmoud (2016) presented an analytical solution for the effect of initial stress, rotation, magnetic field and periodic loading in a thermoviscoelastic medium with a spherical cavity. Othman et al. (2017) studied the influence of magnetic field on generalized piezo-thermoelastic rotating medium with two relaxation times. Quintanilla and Racke (2006) compared two different mathematical hyperbolic models in dual-phase-lag, heat conduction proposed by Tzou, and found the parameter regions where stability can be expected. The theory of thermoelasticity with dual phase-lag effects has been used by Roy Choudhuri (2007) to study the problem of one-dimensional disturbance in an elastic half-space with its plane boundary subjected to a constant step input of temperature and zero stress, or a constant step input of stress and zero temperature. Singh et al. (2017) solved the governing equations of transversely isotropic dual-phase-lag, two-temperature thermoelasticity for the surface waves. Ciesielski (2017) discussed the considerations concerning the analytical solution of DPL equation in the one-dimensional bounded domain. Hou and Leung (2009) studied three-dimensional Green's functions for two-phase transversely isotropic piezothermoelastic media. The reflection and refraction of plane quasi-longitudinal waves at an interface of two piezoelectric media under initial stresses discussed by Abd-Alla and Alsheikh (2009). Othman et al. (2014) studied the effect of rotation on micro-polar generalized thermoelasticity with two-temperatures using a dual-phase-lag model.

In the present paper, the dual-phase-lag model is applied to study the effect of rotation on a half-space filled with a piezo-thermoelastic medium. The normal mode analysis is used to obtain an exact analytical solution for the displacement components, the stress, the strain components, the temperature, the electric potential and the electric displacement. Comparison of the results is carried out with those obtained from Lord and Shulman theory, to assess the effect of rotation on wave propagation. The present results may be of interest in the design and construction of different pyro/piezoelectric devices, such as sensors and gyroscopes involving piezoelectric components.

2 Problem formulation

2.1 Basic equations

Consider a homogeneous, generalized piezo-thermoelastic half-space $(x, y, z \geq 0)$, rotating uniformly with an angular velocity about a fixed axis in space with angular velocity $\mathbf{\Omega} = \Omega \mathbf{n}$, where $\mathbf{n}$ is a unit vector Fig. 1. All considered functions depend on the time variable t and the spatial coordinates x and z. The equation of motion has two additional terms representing Coriolis force and the centripetal acceleration (Schoenberg and Censor 1973). In what follows, we consider a rotation about the y-axis, so that $\mathbf{\Omega} = (0, \Omega, 0)$.

The governing two-dimensional field equations for a homogeneous, generalized anisotropic piezo-thermoelastic solid belonging to a hexagonal crystallographic symmetry class are expressed as (see Sharma and Kumar 2000):

1. Strain-displacement relations

$$\varepsilon_{i,j} = \frac{1}{2}\left(u_{i,j} + u_{j,i}\right). \tag{1}$$

2. Generalized Hooke's law

$$\sigma_{ij} = C_{ijkl}\varepsilon_{kl} - e_{kij}E_k - \beta_{ij}T \tag{2}$$

3. Equation of motion

$$\rho\{\ddot{u}_i + \mathbf{\Omega} \times (\mathbf{\Omega} \times \mathbf{u}) + (2\mathbf{\Omega} \times \dot{\mathbf{u}})_i = \sigma_{ij,j} \tag{3}$$

4. Equation of electrostatics

$$D_{i,i} = 0, \tag{4}$$

5. Electric constitutive equation

$$D_i = e_{ijk}\varepsilon_{jk} + \epsilon_{ij}E_j + p_iT \tag{5}$$
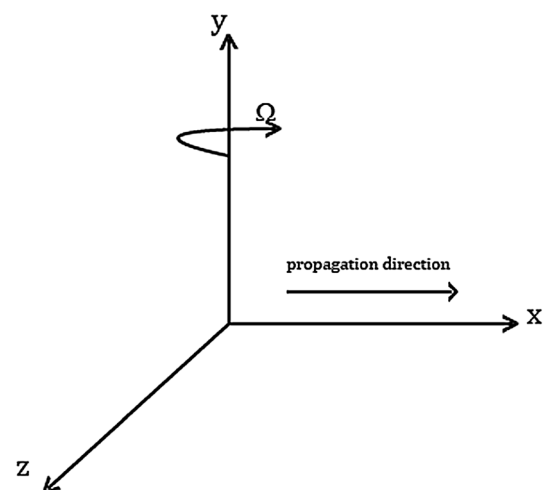
with

Fig. 1 Geometry of the problem and direction of rotation

$$E_i = -\varphi_{,i}, \tag{6}$$

φ being the electric potential.

6. Heat conduction equation in dual-phase-lag model for a piezoelectric material may be expressed as (see Tzou 1995, Aouadi 2006):

$$\left(1 + \tau_\theta \frac{\partial}{\partial t}\right) k_{ij} T_{,ij} = \left(1 + \tau_q \frac{\partial}{\partial t}\right) [\rho C_T \dot{T} + T_0(\beta_{ij} \dot{u}_{i,j} - P_i \dot{\varphi}_{,i})]. \tag{7}$$

In the following, we denote $C_{1111}, C_{1133}, C_{3333}, C_{2323}$ by $C_{11}, C_{13}, C_{33}, C_{44}$ respectively for simplicity.

For the hexagonal (6 mm) crystallographic class under consideration, the constitutive relations are given in components by (Sharma and Kumar 2000) as:

$$\sigma_{xx} = C_{11} \varepsilon_{xx} + C_{13} \varepsilon_{zz} - e_{31} E_z - \beta_1 T, \tag{8}$$

$$\sigma_{zz} = C_{13} \varepsilon_{xx} + C_{33} \varepsilon_{zz} - e_{33} E_z - \beta_3 T, \tag{9}$$

$$\sigma_{xz} = 2C_{44} \varepsilon_{xz} - e_{15} E_x, \tag{10}$$

$$D_x = e_{15}(u_{,z} + w_{,x}) + \epsilon_{11} E_x, \tag{11}$$

$$D_z = e_{31} u_{,x} + e_{33} w_{,z} + \epsilon_{33} E_z + P_3 T. \tag{12}$$

2.2 Boundary conditions

The governing equations will be solved in a half-space $(x, y, z \geq 0)$ under the following boundary conditions:

1. Mechanical boundary conditions:

$$\sigma_{zz}(x, 0, t) = f_1(x, t) = -f_1^* e^{ia(x-ct)}, \qquad \sigma_{xz}(x, 0, t) = 0, \tag{13}$$

2. Thermal boundary condition:

$$T(x, 0, t) = f_2(x, t) = f_2^* e^{ia(x-ct)}, \tag{14}$$

where $f_1(x, t)$ and $f_2(x, t)$ are arbitrary functions of (x, t), f_1^*, f_2^* are constants, a is the wave number in the x-direction and $\omega = ac$ is the frequency.

3. Electrical boundary condition:

$$\frac{\partial \varphi}{\partial z}(x, 0, t) = 0. \tag{15}$$

We consider a homogeneous, anisotropic, piezo-thermoelastic half-space of hexagonal type under the influence of the rotation.

The basic system of field equations (3), (4) and (7) for temperature change $T(x, z, t)$, displacement vector $\mathbf{u}(x, z, t) = (u, 0, w)$, and electric potential $\varphi(x, z, t)$, is given by:

$$C_{11} u_{,xx} + C_{44} u_{,zz} + (C_{13} + C_{44}) w_{,xz} + (e_{31} + e_{15}) \varphi_{,xz} - \beta_1 T_{,x} = \rho(\ddot{u} - \Omega^2 u + 2\Omega \dot{w}), \tag{16}$$

$$(C_{13} + C_{44}) u_{,xz} + C_{44} w_{,xx} + C_{33} w_{,zz} + e_{15} \varphi_{,xx} + e_{33} \varphi_{,zz} - \beta_3 T_{,z} = \rho(\ddot{w} - \Omega^2 w - 2\Omega \dot{u}), \tag{17}$$

$$(e_{15} + e_{31}) u_{,xz} + e_{15} w_{,xx} + e_{33} w_{,zz} - \epsilon_{11} \varphi_{,xx} - \epsilon_{33} \varphi_{,zz} + P_3 T_{,z} = 0, \tag{18}$$

$$\left(1 + \tau_\theta \frac{\partial}{\partial t}\right)(k_1 T_{,xx} + k_3 T_{,zz}) = \left(1 + \tau_q \frac{\partial}{\partial t}\right) [\rho C_T \dot{T} + T_0(\beta_1 \dot{u}_{,x} + \beta_3 \dot{w}_{,z} - P_3 \dot{\varphi}_{,z})] \tag{19}$$

The following non-dimensional quantities are introduced for convenience:

$$x' = \frac{\omega^*}{v_p} x, \quad z' = \frac{\omega^*}{v_p} z, \quad u' = \frac{\rho \omega^* v_p}{\beta_1 T_o} u, \quad w' = \frac{\rho \omega^* v_p}{\beta_1 T_o} w,$$

$$T' = \frac{T}{T_o}, \quad \sigma'_{ij} = \frac{\sigma_{ij}}{\beta_1 T_o}, \quad \varphi' = \varepsilon_p \varphi, \quad \{t', \tau'_\theta, \tau'_q\} = \omega^* \{t, \tau_\theta, \tau_q\},$$

$$D'_i = \frac{D_i}{e}, \quad \Omega' = \frac{\Omega}{\omega^*},$$

where

$$\omega^* = \frac{C_T C_{11}}{K_{11}}, \quad \varepsilon_p = \frac{\omega^* e_{33}}{v_p} \beta_1 T_0,$$

$$\beta_1 = (C_{11} + C_{12}) \alpha_1 + C_{13} \alpha_3, \quad \beta_3 = 2C_{13} \alpha_1 + C_{33} \alpha_3.$$

Using the non-dimensional quantities, system (16)–(19) recasts in the following form after suppressing the primes

$$\delta_1 u_{,xx} + \delta_2 u_{,zz} + \delta_3 w_{,xz} + \delta_4 \varphi_{,xz} - T_{,x} = \ddot{u} - \Omega^2 u + 2\Omega \dot{w} \tag{20}$$

$$\delta_3 u_{,xz} + \delta_2 w_{,xx} + \delta_5 w_{,zz} + \delta_6 \varphi_{,xx} + \varphi_{,zz} + \delta_7 T_{,z} = \ddot{w} - \Omega^2 w - 2\Omega \dot{u} \tag{21}$$

$$\delta_8 u_{,xz} + \delta_9 w_{,xx} + \delta_{10} w_{,zz} + \delta_{11} \varphi_{,xx} + \delta_{12} \varphi_{,zz} + \delta_{13} T_{,z} = 0 \tag{22}$$

$$\left(1 + \tau_\theta \frac{\partial}{\partial t}\right)(\delta_{14} T_{,xx} + \delta_{15} T_{,zz}) = \left(1 + \tau_q \frac{\partial}{\partial t}\right)(\dot{T} + \delta_{16} \dot{u}_{,x} + \delta_{17} \dot{w}_{,z} - \delta_{18} \dot{\varphi}_{,z}) \tag{23}$$

3 Solution of the problem

The solution of the considered physical quantities can be decomposed in terms of normal modes in the following form

$$[u, w, \varphi, T](x, z, t) = [u^*, w^*, \varphi^*, T^*](z)e^{ia(x-ct)}, \tag{24}$$

where u^*, w^*, φ^* and T^* are the amplitudes of the functions u, w, φ and T, respectively. Thus our solution represents progressive waves propagating parallel to the boundary of the half-space, with amplitude decaying in depth.

Substituting from Eq. (24) into Eqs. (20)–(23), and denoting $D = \frac{d}{dz}$, we get

$$(D^2 + A_1)u^* + (A_2D + A_3)w^* \\ + A_4D\varphi^* + A_5T^* = 0, \tag{25}$$

$$(A_6D + A_7)u^* + (D^2 + A_8)w^* + (A_9D^2 \\ + A_{10})\varphi^* + A_{11}DT^* = 0, \tag{26}$$

$$A_{12}Du^* + (D^2 + A_{13})w^* \\ + (A_{14}D^2 + A_{15})\varphi^* + A_{16}DT^* = 0, \tag{27}$$

$$A_{17}u^* + A_{18}Dw^* \\ + A_{19}D\varphi^* + (D^2 + A_{20})T^* = 0. \tag{28}$$

where $A_j, \ j = 1, 2, \ldots, 20$ are given in Appendix A

Equations (25)–(28) have a non-trivial solution only if the determinant of the coefficients of the above linear system vanishes. Then

$$(D^8 - AD^6 + BD^4 - CD^2 + E)\{u^*(z), w^*(z), \\ \varphi^*(z), T^*(z)\} = 0, \tag{29}$$

where $A, \ B, \ C$ and E are given in Appendix A.

Equation (29) can be factored as:

$$(D^2 - k_1^2)(D^2 - k_2^2)(D^2 - k_3^2)(D^2 - k_4^2)\{u^*(z), \\ w^*(z), \varphi^*(z), T^*(z)\} = 0. \tag{30}$$

The solutions of equations (29), which are bounded as $z \to \infty$ are given as:

$$u^* = \sum_{n=1}^{4} M_n e^{-k_n z}, \tag{31}$$

$$w^* = \sum_{n=1}^{4} H_{1n} M_n e^{-k_n z}, \tag{32}$$

$$\varphi^* = \sum_{n=1}^{4} H_{2n} M_n e^{-k_n z}, \tag{33}$$

$$T^* = \sum_{n=1}^{4} H_{3n} M_n e^{-k_n z}, \tag{34}$$

where $k_n^2, (n = 1, 2, 3, 4)$ are the roots of the characteristic equation of Eq. (29).

Inserting Eqs. (31)–(34) into Eqs. (8)–(12), after making dimension analysis, in the frame of the normal mode method, one obtains

$$\sigma_{xx}^* = \sum_{n=1}^{4} H_{4n} M_n e^{-k_n z}, \tag{35}$$

$$\sigma_{zz}^* = \sum_{n=1}^{4} H_{5n} M_n e^{-k_n z}, \tag{36}$$

$$T_{xz}^* = \sum_{n=1}^{4} H_{6n} M_n e^{-k_n z}, \tag{37}$$

$$D_x^* = \sum_{n=1}^{4} H_{7n} M_n e^{-k_n z}, \tag{38}$$

$$D_z^* = \sum_{n=1}^{4} H_{8n} M_n e^{-k_n z}, \tag{39}$$

where $H_{jn}, j = 1, \ldots, 8, n = 1, 2, 3, 4$ are given in Appendix B.

Applying the boundary conditions (13)–(15) to determine the coefficients $M_n(n = 1, 2, 3, 4)$, we obtain

$$\sum_{n=1}^{4} H_{5n} M_n = -f_1^*, \tag{40}$$

$$\sum_{n=1}^{4} H_{6n} M_n = 0, \tag{41}$$

$$\sum_{n=1}^{4} H_{3n} M_n = f_2^*, \tag{42}$$

$$\sum_{n=1}^{4} k_n H_{2n} M_n = 0. \tag{43}$$

Solving Eqs. (40)–(43) for $M_n(n = 1, 2, 3, 4)$ by the inverse matrix method as follows:

$$\begin{pmatrix} M_1 \\ M_2 \\ M_3 \\ M_4 \end{pmatrix} = \begin{pmatrix} H_{51} & H_{52} & H_{53} & H_{54} \\ H_{61} & H_{62} & H_{63} & H_{64} \\ H_{31} & H_{32} & H_{33} & H_{34} \\ k_1 H_{21} & k_2 H_{22} & k_3 H_{23} & k_4 H_{24} \end{pmatrix}^{-1} \begin{pmatrix} -f_1^* \\ 0 \\ f_2^* \\ 0 \end{pmatrix} \tag{44}$$

Thus, we obtain an exact analytical formula for the displacement vector components, the stress and the strain tensors components, the temperature, the electric potential and the electric displacement.

4 Numerical results and discussion

To study the effect of rotation, we will carry out some numerical experiments. The material chosen for the purpose of the numerical calculations is taken as Cadmium Selenide (CdSe) having hexagonal symmetry (6 mm class).

The following particular values for the parameters are chosen as:

$C_{11} = 7.41 \times 10^{10} \, \text{Nm}^{-2}, \quad C_{12} = 4.52 \times 10^{10} \, \text{Nm}^{-2},$

$C_{13} = 3.93 \times 10^{10} \, \text{Nm}^{-2}, \quad C_{33} = 8.36 \times 10^{10} \, \text{Nm}^{-2},$

$C_{44} = 1.32 \times 10^{10} \, \text{Nm}^{-2}, \quad T_0 = 298 \, \text{K},$

$\rho = 5504 \, \text{kg m}^{-3}, \quad C_T = 260 \, \text{J kg}^{-1} \, \text{K}^{-1}.$

$e_{13} = -0.160 \, \text{Cm}^{-2}, \quad e_{33} = 0.347 \, \text{Cm}^{-2},$

$\quad e_{15} = -0.138 \, \text{Cm}^{-2},$

$\beta_1 = 0.621 \times 10^6 \, \text{Nk}^{-1} \, \text{m}^{-2},$

$\quad \beta_3 = 0.551 \times 10^6 \, \text{Nk}^{-1} \, \text{m}^{-2},$

$P_3 = -2.94 \times 10^6 \, \text{Ck}^{-1} \, \text{m}^{-2},$

$\quad K_1 = K_3 = 9 \, \text{Wm}^{-1} \, \text{K}^{-1},$

$\epsilon_{11} = 8.26 \times 10^{-11} \text{C}^2 \text{N}^{-1} \, \text{m}^{-2},$

$\quad \epsilon_{33} = 9.03 \times 10^{-11} \text{C}^2 \text{N}^{-1} \, \text{m}^{-2}.$

$\tau_q = 0.9342 \times 10^{-12} \, \text{s},$

$\tau_\theta = 0.37371 \times 10^{-12} \, \text{s}.$

For these values, the characteristic time

$$\frac{1}{\omega^*} \simeq 0.4671 \times 10^{-12} \, \text{s}$$

is in the range of picoseconds, while the characteristic length is

$$\frac{v_p}{\omega^*} \simeq 0.1714 \times 10^{-8} \, \text{m}.$$

In applying the numerical technique outlined above, we are interested in the real parts of the displacement vector components u, w, the temperature T, the stress tensor components $\sigma_{xx}, \sigma_{zz}, \sigma_{xz}$, the electric potential φ and the electric displacement components D_x, D_z. Here all variables are taken in non-dimensional form. The results are shown in Figs. 2, 3, 4, 5, 6, 7, 8, 9 and 10. The graphs exhibit the curves predicted by L–S theory and DPL model. In these figures, the solid lines represent the solution in the dual-phase-lag model and dashed lines represent the solution derived using the generalized Lord and Shulman theory.

These figures show a comparison between the values assumed by the different functions of practical interest in the absence of rotation ($\Omega = 0$) and for $\Omega = 0.4$. Comparison is also carried out between the results of DPL and those from L–S. The computations are carried out for the non-dimensional instant of time $t = 1.5$ at $x = 0.1$ with $f_1^* = 1$ and $f_2^* = 6$. It follows from the presented figures that all the physical quantities suffer appreciable variations only in a narrow slab $0 \leq z \leq 1$, while all quantities practically vanish outside the slab $0 \leq z \leq 2$.
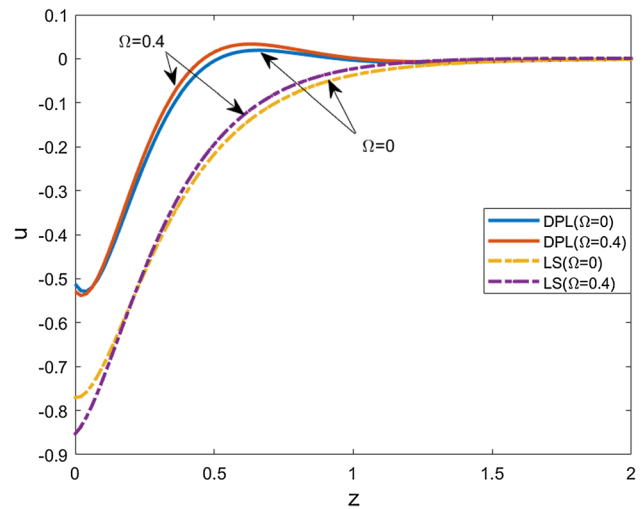

Fig. 2 Distribution of the horizontal component u of the displacement vector at $x = 0.1$, $t = 1.5$, in the absence or presence of rotation
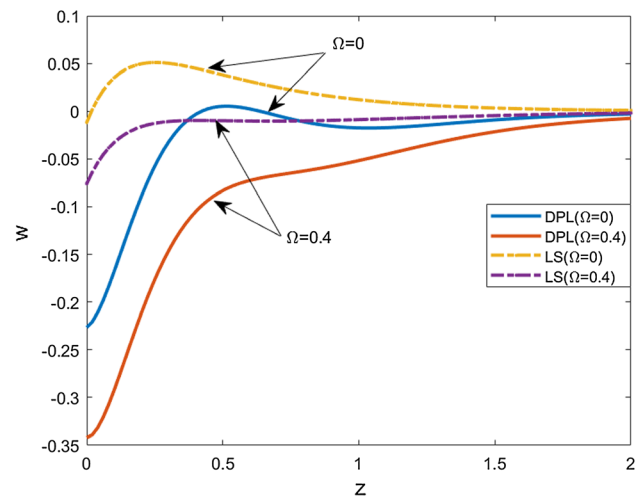

Fig. 3 Distribution of the vertical component w of the displacement vector at $x = 0.1$, $t = 1.5$, in the absence or presence of rotation

Figure 2 depicts the distribution of the displacement u parallel to the boundary against z. It shows that this displacement component wealky depends on rotation, which amounts to adding a small positive displacement, and is for the most part opposite to the direction of propagation of the wave. The absolute value of this displacement component for L–S is monotonically decreasing, and exceeds that obtained from DPL.

Figure 3 illustrates the distribution of the in-depth displacement w against z. Here, the effect of rotation is appreciable, and amounts to adding a negative displacement. Moreover, the absolute values obtained for this displacement component are larger with DPL.

Figure 4 exhibits the behavior of temperature T against z. As expected, the effect of rotation here is negligible. The temperature for L–S is monotonic decreasing to zero, and
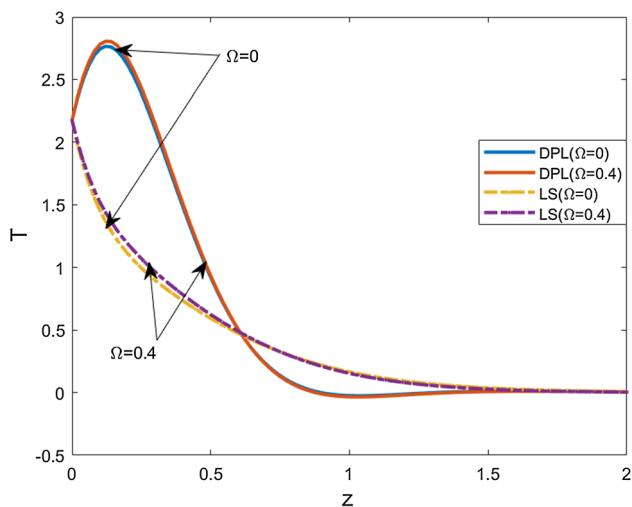
Fig. 4 Temperature distribution T at $x = 0.1$, $t = 1.5$, in the absence or presence of rotation
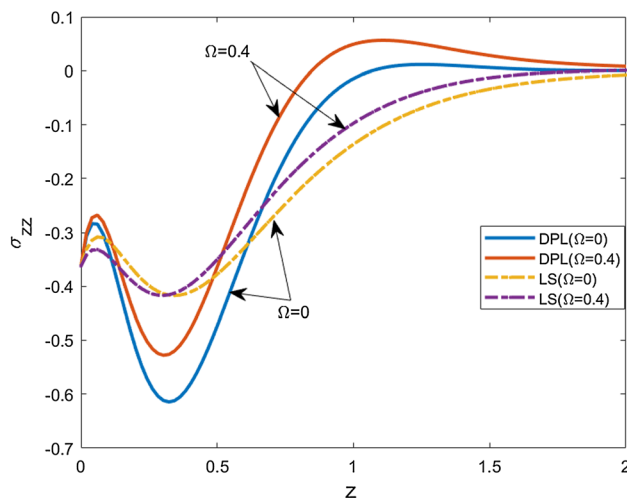

Fig. 6 Distribution of the stress component σ_{zz} at $x = 0.1$, $t = 1.5$, in the absence or presence of rotation
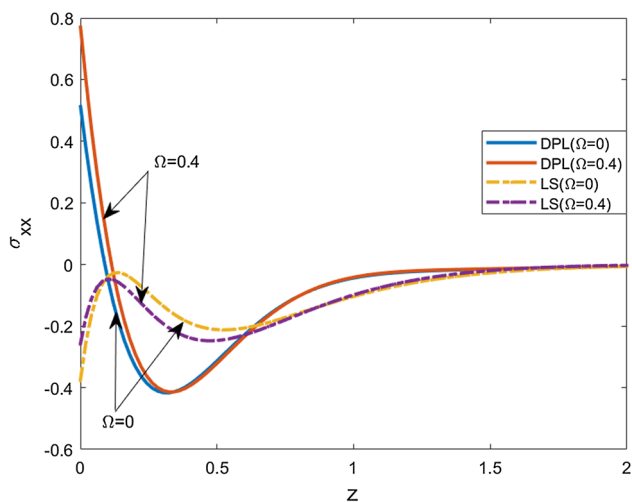

Fig. 5 Distribution of the stress component σ_{xx} at $x = 0.1$, $t = 1.5$, in the absence or presence of rotation
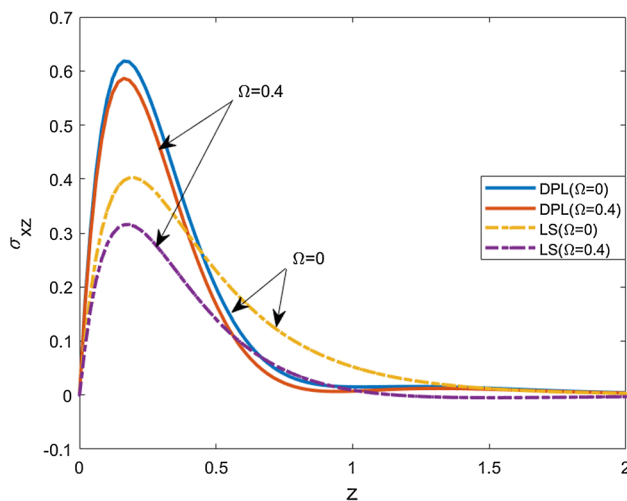

Fig. 7 Distribution of the stress component σ_{xz} at $x = 0.1$, $t = 1.5$, in the absence or presence of rotation

is smaller than that obtained from DPL in the neighborhood of the boundary.

Figures 5, 6 and 7 show the distributions of the stress tensor components $\sigma_{xx}, \sigma_{zz}, \sigma_{xz}$ with z. The effect of rotation is appreciable only for the last two components, while the fluctuations of the three stress components are more appreciable for DPL than for L–S.

Figures 8, 9 and 10 exhibit the distributions with z of the electrical potential φ and the two electric displacement components D_x and D_z. The effect of rotation is appreciable only for φ and D_x within DPL, while it is negligible otherwise. Here again, the fluctuations within DPL are

more pronounced for the first two functions as compared to the corresponding results of L–S.

Figures 11, 12, 13, 14, 15, 16, 17, 18 and 19 exhibit the 3D plots of the solution in the (x, z) plane at $t = 1.5$ for DPL, in the presence of rotation ($\Omega = 0.4$).

5 Conclusions

The main purpose of the present work is to assess the effect of rotation on a piezo-thermoelastic medium within dual-phase-lag model. Comparison is carried out with the results obtained from L–S. Normal mode analysis is used for the
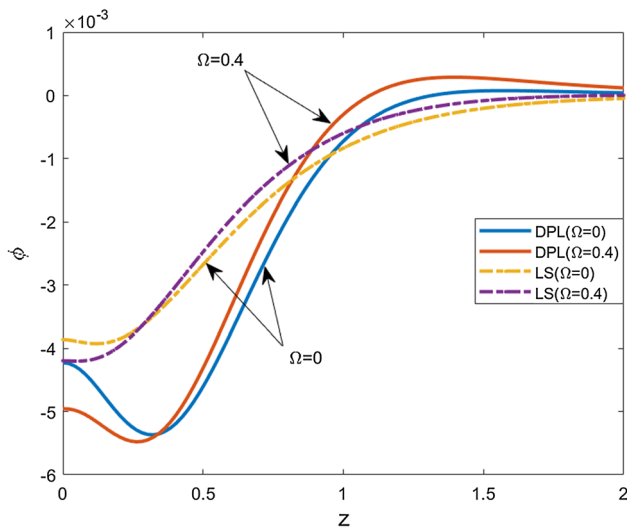
Fig. 8 Distribution of the electric potential φ at $x = 0.1$, $t = 1.5$, in the absence or presence of rotation
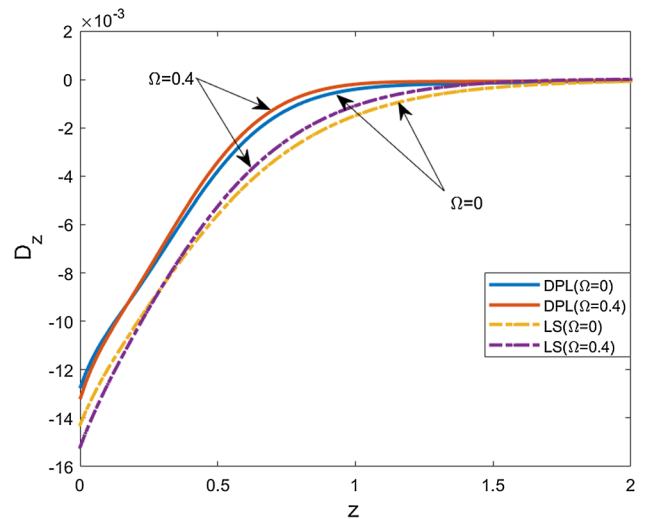

Fig. 10 Distribution of the electric displacement component D_z at $x = 0.1$, $t = 1.5$, in the absence or presence of rotation
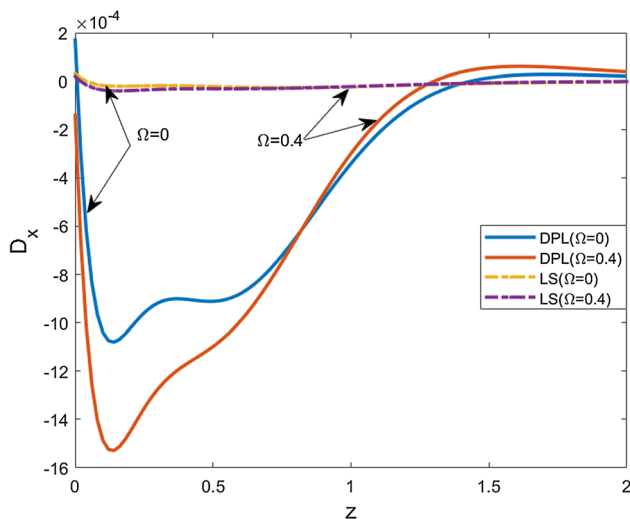

Fig. 9 Distribution of the electric displacement component D_x at $x = 0.1$, $t = 1.5$, in the absence or presence of rotation
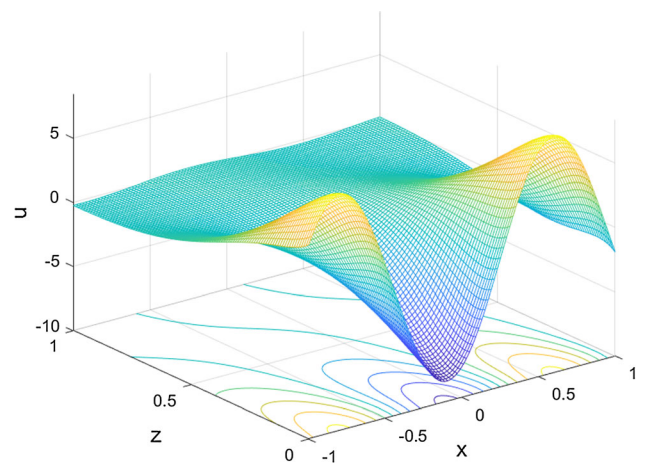

Fig. 11 The distribution of the horizontal component u of the displacement vector at $t = 1.5$ in the (x, z) plane calculated in the frame of the DPL model with $\Omega = 0.4$

solution of the mathematical problem, and the boundary conditions are particulary chosen to fit the requirements of such technique.

An exact analytical solution is obtained under these limitations. According to this solution, all the physical quantities tend to zero away from the boundary and all functions are continuous.

The performed calculations at particular locations of the half-space have revealed that the effect of rotation may differ from one physical quantity to the other, and that fluctuations of the different functions in the zone near the boundary are more pronounced within DPL, than those obtained from the L–S theory.

The presented results, in connection with experimental measurements, may be useful in calculating numerical values of different material parameters, and in assessing the efficiency of the two considered theories.

A numerical treatment of the general system of equations and conditions governing the phenomenon may be useful in getting rid of the limitations of the method of normal modes' technique and this task is actually in progress.
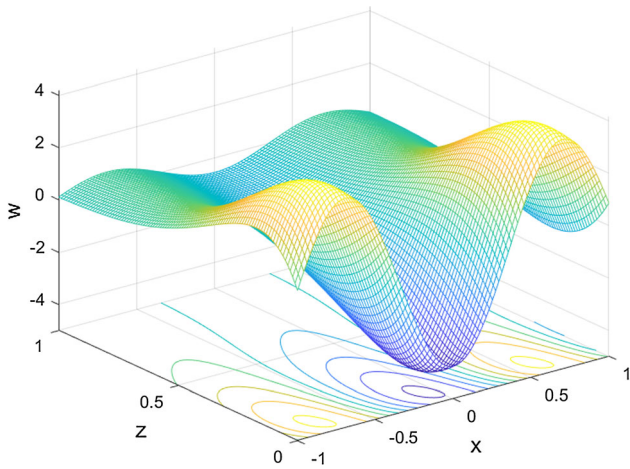
Fig. 12 Distribution of the vertical component w of the displacement vector at $t = 1.5$ in the (x, z) plane calculated in the frame of the DPL model with $\Omega = 0.4$
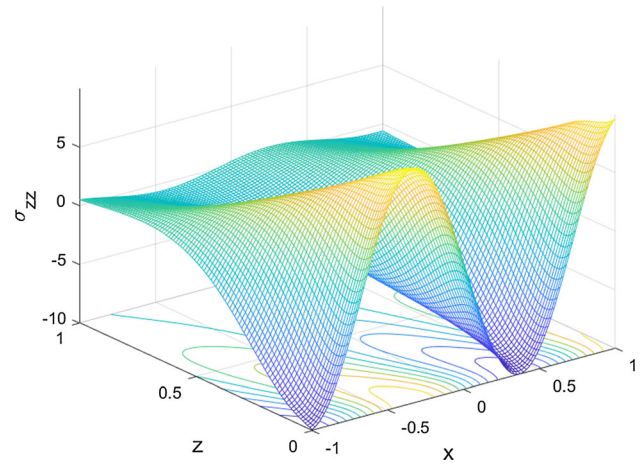

Fig. 15 Distribution of the stress component σ_{zz} at $t = 1.5$ in the (x, z) plane calculated in the frame of the DPL model with $\Omega = 0.4$
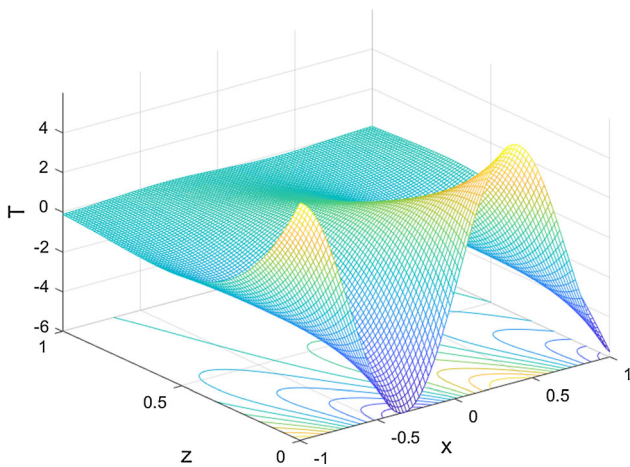

Fig. 13 Distribution of the temperature T at $t = 1.5$ in the (x, z) plane calculated in the frame of the DPL model with $\Omega = 0.4$
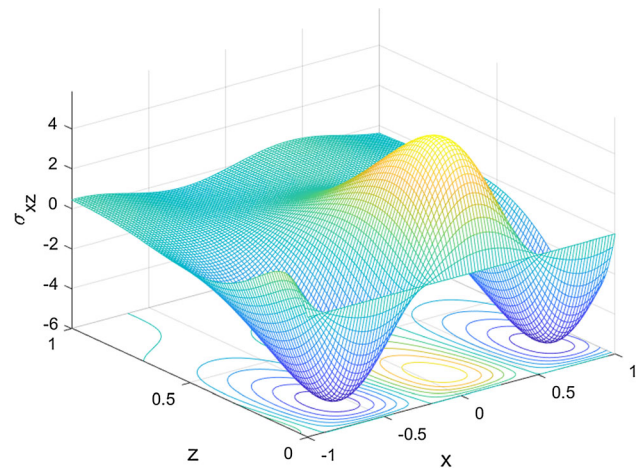

Fig. 16 Distribution of the stress component σ_{xz} at $t = 1.5$ in the (x, z) plane calculated in the frame of the DPL model with $\Omega = 0.4$
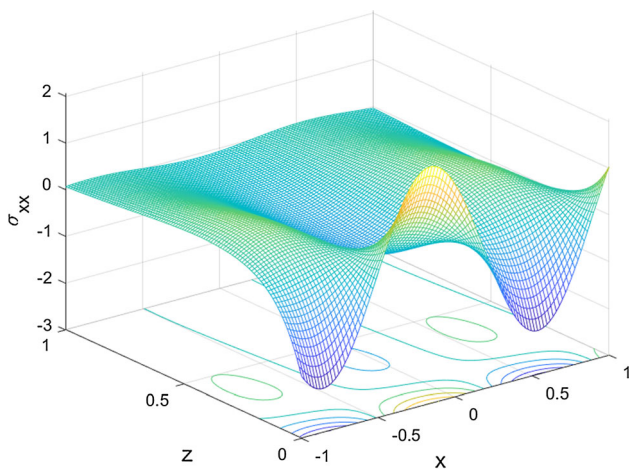

Fig. 14 Distribution of the stress component σ_{xx} at $t = 1.5$ in the (x, z) plane calculated in the frame of the DPL model with $\Omega = 0.4$
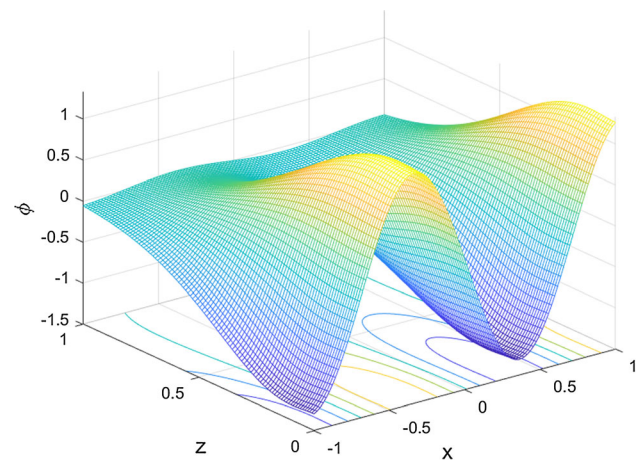

Fig. 17 Distribution of the electric potential φ at $t = 1.5$ in the (x, z) plane calculated in the frame of the DPL model with $\Omega = 0.4$
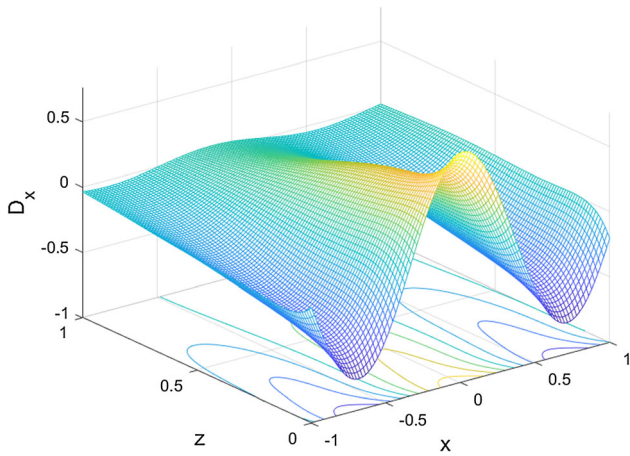
Fig. 18 Distribution of the electric displacement component D_x at $t = 1.5$ in the (x, z) plane calculated in the frame of the DPL model with $\Omega = 0.4$
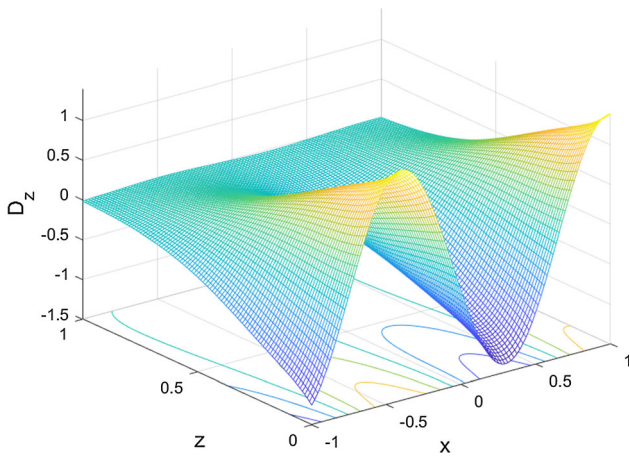

Fig. 19 Distribution of the electric displacement component D_z at $t = 2.0$ in the (x, z) plane calculated in the frame of the DPL model at $t = 1.5$ with $\Omega = 0.4$

Appendices

Appendix A

$$\delta_1 = \frac{C_{11}}{\rho v_p^2}, \delta_2 = \frac{C_{44}}{\rho v_p^2},$$

$$\delta_3 = \frac{(C_{13} + C_{44})}{\rho v_p^2}, \delta_4 = \frac{(e_{31} + e_{15})}{e_{33}}, \delta_5 = \frac{C_{33}}{\rho v_p^2},$$

$$\delta_6 = \frac{e_{15}}{e_{33}}, \delta_7 = -\frac{\beta_3}{\beta_1},$$

$$\delta_8 = \frac{(e_{15} + e_{31})}{\rho v_p^2}, \delta_9 = \frac{e_{15}}{\rho v_p^2},$$

$$\delta_{10} = \frac{e_{33}}{\rho v_p^2},$$

$$\delta_{11} = -\frac{\epsilon_{11}}{e_{33}}, \delta_{12} = -\frac{\epsilon_{33}}{e_{33}},$$

$$\delta_{13} = \frac{P_3}{\beta_1}, \delta_{14} = \frac{K_1 \omega^*}{\rho C_T v_p^2},$$

$$\delta_{15} = \frac{K_3 \omega^*}{\rho C_T v_p^2},$$

$$\delta_{16} = \frac{\beta_1^2 T_0}{\rho^2 C_T v_p^2}, \delta_{17} = \frac{\beta_1 \beta_3 T_0}{\rho^2 C_T v_p^2},$$

$$\delta_{18} = -\frac{P_3 \beta_1 T_0}{\rho C_T e_{33}}.$$

and

$$A_1 = \frac{a^2 c^2 - a^2 \delta_1 + \Omega^2}{\delta_2}, \quad A_2 = \frac{ia\delta_3}{\delta_2}, \quad A_3 = \frac{2iac\Omega}{\delta_2},$$

$$A_4 = \frac{ia\delta_4}{\delta_2}, \quad A_5 = \frac{-ia}{\delta_2}, \quad A_6 = \frac{ia\delta_3}{\delta_5}, \quad A_7 = \frac{-2iac\Omega}{\delta_5},$$

$$A_8 = \frac{a^2 c^2 - a^2 \delta_2 + \Omega^2}{\delta_5}, \quad A_9 = \frac{1}{\delta_5}, \quad A_{10} = -\frac{a^2 \delta_6}{\delta_5},$$

$$A_{11} = \frac{\delta_7}{\delta_5}, \quad A_{12} = \frac{ia\delta_8}{\delta_{10}}, \quad A_{13} = -\frac{a^2 \delta_9}{\delta_{10}}, \quad A_{14} = \frac{\delta_{12}}{\delta_{10}},$$

$$A_{15} = -\frac{a^2 \delta_{11}}{\delta_{10}}, \quad A_{16} = \frac{\delta_{13}}{\delta_{10}}, \quad A_{17} = -\frac{a^2 c\delta_{16}(1 - iac\tau_q)}{\delta_{15}(1 - iac\tau_\theta)},$$

$$A_{18} = \frac{iac\delta_{17}(1 - iac\tau_q)}{\delta_{15}(1 - iac\tau_\theta)},$$

$$A_{19} = \frac{iac\delta_{18}(1 - iac\tau_q)}{\delta_{15}(1 - iac\tau_\theta)},$$

$$A_{20} = \frac{-a^2 \delta_{14}(1 - iac\tau_\theta) + iac(1 - iac\tau_q)}{\delta_{15}(1 - iac\tau_\theta)},$$

$$\begin{aligned} A = \frac{-1}{A_{14} - A_9} (&A_{14}A_{20} + A_{15} - A_{16}A_{19} + A_8 A_{14} \\ &- A_9 A_{20} - A_9 A_{13} A_9 A_{16} A_{18} - A_{10} + A_{11} A_{19} \\ &- A_{11} A_{14} A_{18} + A_1 A_{14} - A_1 A_{19} A_2 A_6 A_{14} \\ &+ A_2 A_9 A_{12} + A_4 A_6 - A_4 A_{12}), \end{aligned}$$

$$\begin{aligned} B = \frac{1}{(A_{14} - A_9)} (&A_5 A_{20} + A_8 A_{14} A_{20} + A_8 A_{15} \\ &- A_8 A_{16} A_{19} - A_9 A_{13} A_{20} - A_{10} A_{13} \\ &+ A_{10} A_{20} + A_{10} A_{16} A_{18} + A_{11} A_{13} A_{19} - A_{11} A_{15} A_{18} \\ &+ A_1 A_{14} A_{20} + A_1 A_{15} - A_1 A_{16} A_{19} \\ &+ A_1 A_8 A_{14} - A_1 A_9 A_{13} - A_1 A_9 A_{20} \\ &+ A_1 A_9 A_{16} A_{18} - A_1 A_{10} + A_1 A_{11} A_{19} \\ &- A_1 A_{11} A_{14} A_{18} - A_2 A_6 A_{14} A_{20} - A_2 A_6 A_{15} \\ &+ A_2 A_6 A_{16} A_{19} + A_2 A_9 A_{12} A_{20} - A_2 A_9 A_{16} A_{17} \\ &+ A_2 A_{10} A_{12} - A_2 A_{11} A_{12} A_{19} + A_2 A_{11} A_{14} A_{17} - A_3 A_7 A_{14} \\ &+ A_4 A_6 A_{13} + A_4 A_6 A_{20} - A_4 A_6 A_{16} A_{18} - A_4 A_{12} A_{20} \\ &+ A_4 A_{16} A_{17} - A_4 A_8 A_{12} + A_4 A_{11} A_{12} A_{18} - A_4 A_{11} A_{17} \\ &+ A_5 A_6 A_{19} + A_5 A_6 A_{14} A_{18} + A_5 A_{12} A_{19} \\ &- A_5 A_{14} A_{17} - A_5 A_9 A_{12} A_{18} + A_5 A_9 A_{17}), \end{aligned}$$

$$C = \frac{-1}{(A_{14} - A_9)}(A_8 A_{15} A_{20} - A_{10} A_{13} A_{20} + A_1 A_{15} A_{20}$$
$$+ A_1 A_8 A_{14} A_{20} + A_1 A_8 A_{15} - A_1 A_8 A_{16} A_{19}$$
$$- A_1 A_9 A_{13} A_{20} - A_1 A_{10} A_{13} - A_1 A_{10} A_{20}$$
$$+ A_1 A_{10} A_{16} A_{18} + A_1 A_{11} A_{13} A_{19} - A_1 A_{11} A_{15} A_{18}$$
$$- A_2 A_6 A_{15} A_{20} + A_2 A_{10} A_{12} A_{20} - A_2 A_{10} A_{16} A_{17}$$
$$+ A_2 A_{11} A_{15} A_{17} - A_3 A_7 A_{14} A_{20} - A_3 A_7 A_{15}$$
$$+ A_3 A_7 A_{16} A_{19} + A_4 A_6 A_{13} A_{20} - A_4 A_8 A_{12} A_{20}$$
$$+ A_4 A_8 A_{16} A_{17} - A_4 A_{11} A_{13} A_{17} - A_5 A_6 A_{13} A_{19}$$
$$+ A_5 A_6 A_{15} A_{18} - A_5 A_{15} A_{17} + A_5 A_8 A_{12} A_{19}$$
$$- A_5 A_8 A_{14} A_{17} + A_5 A_9 A_{13} A_{17} - A_5 A_{10} A_{12} A_{18}$$
$$+ A_5 A_{10} A_{17}),$$
$$E = \frac{1}{(A_{14} - A_9)}(A_1 A_8 A_{15} A_{20} - A_1 A_{10} A_{13} A_{20}$$
$$- A_3 A_7 A_{15} A_{20} - A_5 A_8 A_{15} A_{17} + A_5 A_{10} A_{13} A_{17}).$$

Appendix B

$$H_{1n} = -\frac{s_{1n}}{s_{2n}},$$
$$H_{2n} = -\frac{q_{1n} + q_{2n} H_{1n}}{q_{3n}},$$
$$H_{3n} = -\frac{(k_n^2 + A_1) + (-A_2 k_n + A_3) H_{1n} - A_4 k_n H_{2n}}{A_5},$$
$$H_{4n} = [r_1 - l_1 k_n H_{1n} - l_2 k_n H_{2n} - H_{3n}],$$
$$H_{5n} = [r_2 - \delta_5 k_n H_{1n} - k_n H_{2n} + \delta_7 H_{3n}],$$
$$H_{6n} = [-\delta_2 k_n + r_3 H_{1n} + r_4 H_{2n}],$$
$$H_{7n} = [-l_3 k_n + r_5 H_{1n} + r_6 H_{2n}],$$
$$H_{8n} = [r_7 - l_6 k_n H_{1n} - l_7 k_n H_{2n} + l_8 H_{3n}].$$
$$n = 1, 2, 3, 4.$$
$$q_{1n} = A_{11} k_n^3 + (A_1 A_{11} - A_5 A_6) k_n + A_5 A_7,$$
$$q_{2n} = (-A_2 A_{11} + A_5) k_n^2 + A_3 A_{11} k_n + A_5 A_8,$$
$$q_{3n} = (-A_4 A_{11} + A_5 A_9) k_n^2 + A_5 A_{10},$$
$$q_{4n} = A_{16} k_n^3 + (A_1 A_{16} - A_5 A_{12}) k_n,$$
$$q_{5n} = (A_5 - A_2 A_{16}) k_n^2 + A_3 A_{16} k_n + A_5 A_{13},$$
$$q_{6n} = (A_5 A_{14} - A_4 A_{16}) k_n^2 + A_5 A_{15}.$$
$$s_{1n} = q_{1n} q_{6n} - q_{3n} q_{4n},$$
$$s_{2n} = q_{2n} q_{6n} - q_{3n} q_{5n}.$$
$$l_1 = \frac{C_{13}}{\rho v_p^2},$$
$$l_2 = \frac{e_{31}}{e_{33}},$$
$$l_3 = \frac{e_{15} \beta_1 T_0}{e \rho v_p^2},$$

$$l_4 = -\frac{\epsilon_{11} \beta_1 T_0}{e e_{33}},$$
$$l_5 = \frac{e_{31} \beta_1 T_0}{e \rho v_p^2},$$
$$l_6 = \frac{e_{33} \beta_1 T_0}{e \rho v_p^2},$$
$$l_7 = -\frac{\epsilon_{33} \beta_1 T_0}{e e_{33}},$$
$$l_8 = -\frac{P_3 T_0}{e}.$$
$$\{r_1, r_2, r_3, r_4, r_5, r_6, r_7\} = ia\{\delta_1, l_1, \delta_2, \delta_6, l_3, l_4, l_5\}$$

References

Abbas IA, Zenkour AM (2014) Dual-phase-lag model on thermoelastic interactions in a semi-infinite medium subjected to a ramp-type heating. J Comput Theor Nanosci 11(3):642–645

Abd-Alla AN, Alsheikh FA (2009) Reflection and refraction of plane quasi-longitudinal waves at an interface of two piezoelectric media under initial stresses. Arch Appl Mech 79(9):843–857

Abou-Dina MS, Dhaba EL, Ghaleb AF, Rawy EK (2017) A model of nonlinear thermo-electroelasticity in extended thermo-electroelasticity in extended thermoelasticity. Int J Eng Sci 119:29–39

Ahmed EAA, Abou-Dina MS, El Dhaba AR (2019) Effect of gravity on piezo-thermoelasticity within the dual-phase-lag model. Microsyst Technol 25:1–10

Alshaikh FA (2012) The mathematical modelling for studying the influence of the initial stresses and relaxation times on reflection and refraction waves in piezothermoelastic half-space. Appl Math 3:819–832

Ciesielski M (2017) Analytical solution of the dual phase lag equation describing the laser heating of thin metal film. J Appl Math Comput Mech 16(1):33–40

Hou PF, Leung AYT (2009) Three-dimensional Green′s functions for two-phase transversely isotropic piezothermoelastic media. J Intell Mater Syst Struct 16(5):1915–1923

Kumar R, Sharma N, Lata P, Marin M (2018) Reflection of plane waves at micropolar piezothermoelastic half-space. CMST 24(1):113–124

Li L, Wei PJ (2014) The piezoelectric and piezomagnetic effect on the surface wave velocity of magneto-electroelastic solids. J Sound Vib 333(8):2312–2326

Mahmoud SR (2016) An analytical solution for the effect of initial stress, rotation, magnetic field and a periodic loading in a thermoviscoelastic medium with a spherical cavity. Mech Adv Mater Struct 23(1):1–7

Mindlin RD (1974) Equations of high frequency vibrations of thermo-piezo-electric plate. Int J Solids Struct 10:625–637

Othman MIA (2004) Effect of rotation on plane waves in generalized thermoelasticity with two relaxation times. Int J Solids Struct 41:2939–2956

Othman MIA, Ahmed EAA (2015) The effect of rotation on piezo-thermoelastic medium using different theories. Struct Eng Mech 56(4):649–665

Othman MIA, Ahmed EAA (2016) Influence of the gravitational field on piezo-thermoelastic rotating medium with G–L theory. Eur Phys J Plus 131:1–12

Othman MIA, Elmaklizi YD, Ahmed EAA (2017) Influence of magnetic field on generalized piezo-thermoelastic rotating medium with two relaxation times. Microsyst Technol 23(12):5599–5612

Othman MIA, Hasona WM, Eraki EEM (2013) Influence of gravity field and rotation on a generalized thermoelastic medium using a dual-phase-lag model. J Thermoelast 1(4):12–22

Othman MIA, Hasona WM, Eraki EEM (2014) Effect of rotation on micro-polar generalized thermoelasticity with two-temperatures using a dual-phase-lag model. Can J Phys 92(2):149–158

Quintanilla R, Racke R (2006) A note on stability of dual-phase-lag heat conduction. Int J Heat Mass Transf 49:1209–1213

Roy Choudhuri SK (2007) One-dimensional thermoelastic waves in elastic half-space with dual phase lag effects. J Mech Mater Struct 2(3):489–503

Schoenberg M, Censor D (1973) Elastic waves in rotating media. Q Appl Math 31:115–125

Sharma JN, Kumar M (2000) Plane harmonic waves in piezo-thermoelastic materials. Indian J Eng Mater Sci 7:434–442

Singh B, Kumari S, Singh J (2017) Propagation of Rayleigh wave in two temperature dual phase lag thermoelasticity. Mech Mech Eng 21(1):105–116